International Journal of Dynamics and Control (2026) 14:161
https://doi.org/10.1007/s40435-026-02094-1

RESEARCH

The Lie group approach for the p-defocusing Klein–Gordon equation

Gulistan Iskenderoglu[1] · **Dogan Kaya**[1]

Received: 15 April 2025 / Revised: 20 January 2026 / Accepted: 28 March 2026
© The Author(s), under exclusive licence to Springer-Verlag GmbH Germany, part of Springer Nature 2026

Abstract

In this work, we investigate the nonlinear p-defocusing Klein–Gordon equation with a general defocusing nonlinearity $f(|q|^2) = (1 + |q|^{p-1})$, where $p > 1$, in two spatial dimensions. We use Lie symmetry analysis to systematically reduce the equation to simpler forms, which allows us to discover invariant solutions and facilitate complex stability analysis. Using Lie group methods, we derive several classes of reduced equations and exact travelling wave solutions. The solutions exhibit localised solitary waves, modulated localised structures (spatially confined waves with internal oscillations), and periodic wave trains depending on the balance between the wave speed, direction, and the nonlinearity parameter p. The stability of these travelling wave solutions is analysed using a linear stability framework that identifies conditions under which the solutions are stable or prone to growth and decay. Dispersion relations, phase velocities, and group velocities are derived to characterise the wave behaviour in detail. We also study the physical implications of the solutions in plasma physics and nonlinear wave dynamics, presenting graphical representations to illustrate their profiles and stability characteristics.

Keywords Lie groups · Klein–Gordon equation · Stability analysis · $(1/G')$-expansion method

1 Introduction

The classical Klein–Gordon (or Klein–Gordon-Fock) equation

$$\frac{1}{c^2}u_{tt} - \Delta u + \frac{m^2c^2}{\hbar^2}u = 0, \tag{1}$$

where m, c, and $\hbar$ are, respectively, the mass, the speed of light, and Planck's constant, plays a crucial role in mathematical physics. It is commonly used to describe fast-moving particles with mass and is applicable in the study of massive scalar fields, such as the Higgs field. Thus, the Klein–Gordon equation for a complex scalar field serves as a relativistic extension of the Schrödinger equation, which describes spinless particles. Originally, Schrödinger considered this equation while seeking to describe de Broglie waves, but he later formulated the well-known Schrödinger equation. This equation was named after the physicists Oskar Klein, Walter Gordon, and Vladimir Fock. In 1926, Fock published a generalisation of this equation to cases involving magnetic fields where forces depend on velocity, deriving it independently [1, 2]. Both Klein and Fock employed the Kaluza–Klein method [3], while Gordon's early 1926 article addressed a Compton effect [4].

It is possible to search for solutions to the Klein–Gordon (Klein–Gordon-Fock) equation (1) for a free particle, as with any linear differential equation with constant coefficients, in the form of a superposition of plane waves:

$$u(t, \mathbf{x}) = e^{i(k\mathbf{x}-\omega t)},$$

yielding the relation:

$$-k^2 + \frac{\omega^2}{c^2} = \frac{m^2c^2}{\hbar^2}.$$

A plane wave describes a pure state with a certain energy and momentum.

On the other hand, the equation describing scalar fields

$$u_{tt} - \Delta u + f(|u|^2)u = 0, \quad \text{on } \mathbb{R} \times \mathbb{R}^n, \tag{2}$$

is known as a generalised nonlinear Klein–Gordon equation. It has special solutions of the form:

✉ Gulistan Iskenderoglu
giskenderoglu@ticaret.edu.tr

Dogan Kaya
dogank@ticaret.edu.tr

[1] Istanbul Ticaret University, Istanbul, Turkey

Published online: 29 April 2026

$u = v(x - ct)$,

where c is a vector in $\mathbb{R}^n$ with $|c| < 1$. Such solutions can provide localised travelling wave solutions exhibiting solitary-wave characteristics. The solitons associated with equation (2) can excite the crystal beyond a threshold amplitude, leading to the nucleation of a soliton lattice. Similar phenomena can be observed in other forms of the Klein–Gordon equation, such as the sine-Gordon and double sine-Gordon equations (see, e.g. [5–12] and references therein).

Polat and Taskesen [13] studied the global existence of solutions for the Cauchy problem of a Klein–Gordon equation with high-energy initial data. Shatah [14, 15] established sufficient conditions for stability in a specific case of (2) with $f(|u|^2)u = (1 - |u|^p)u$ for integer $p > 1$. He demonstrated the stability of standing waves of the form $\mathfrak{F}(x)e^{ict}$, where $\mathfrak{F}(x)$ is a least-energy steady-state solution, when $1 < p < 1 + 4/n$ and $n \geq 3$, provided:

$$\sqrt{\frac{p-1}{4-(n-1)(p-1)}} < |c| < 1.$$

Here, $C = \sqrt{\frac{p-1}{4-(n-1)(p-1)}}$ is the critical frequency. An instability result was also obtained in [15] for $1 + 4/n < p < 1 + 4/(n-2)$. Furthermore, Shatah and Strauss [16] showed that $\mathfrak{F}(x)e^{ict}$ is orbitally unstable when $p \geq 1+4/n$, $n \leq 4/(p-1)$, and $c^2 < 1$, or when $1 < p < 1 + 4/n$, $n \geq 3$ with $|c| < C$.

Although these rigorous analytical results establish fundamental existence and stability criteria for specific power nonlinearities, most previous studies either focus on one-dimensional reductions or employ travelling wave ansätze postulated without systematic justification. A complete classification of invariant solutions via Lie symmetry methods remains largely unexplored for multidimensional Klein–Gordon equations with general defocusing nonlinearities $|q|^{p-1}$, $p > 1$. Such a classification would guarantee exhaustiveness and reveal the underlying group-theoretical structure. Recent advances have demonstrated the effectiveness of systematic Lie group approaches for other nonlinear wave systems [23–28], motivating a similarly rigorous treatment of the defocusing Klein–Gordon case.

These analytical results on existence and stability were mainly developed in a mathematical context. To fully appreciate the significance of such nonlinear wave phenomena, we must consider their relevance in physical systems. The nonlinear Klein–Gordon equation with defocusing nonlinearity naturally emerges in various physical settings. In these contexts, the balance between dispersion and nonlinearity governs the formation and dynamics of wave structures.

In plasma physics, for instance, it models the coupling between Langmuir and ion-acoustic waves in the well-known Klein–Gordon–Zakharov system [6, 8]. In nonlinear optics, it describes ultra-short pulse propagation in defocusing Kerr media and formation of dark solitons [17]. In field theory, defocusing Klein–Gordon-type models like the ϕ^4 and sine-Gordon equations govern topological defects and scalar boson configurations [18, 19]. These applications motivate the study of exact and stable solutions of the p - defocusing nonlinear Klein–Gordon equation in a multidimensional setting.

This work presents new results on Lie symmetries, exact solutions, and the stability of travelling wave solutions for the p-defocusing nonlinear Klein–Gordon (dKG) equation with $f(|u|^2)u = (1 + |u|^{p-1})u$:

$$q_{tt} - \Delta q + q = -|q|^{p-1}q, \tag{3}$$

where $\mathbf{x} \in \mathbb{R}^n$ with $n = 2$, and general defocusing nonlinearity $|q|^{p-1}$, $p > 1$ [20, 21].

Significant efforts have been made to obtain explicit exact solutions using Lie group methods [22–24]. This powerful methodology determines the symmetries of nonlinear systems, enabling systematic reduction and derivation of exact solutions. Its versatility has been demonstrated through applications to other nonlinear equations [23–28]. The present work addresses this gap by providing a complete Lie symmetry classification of equation (3). We derive all admitted point symmetries systematically rather than postulating them a priori. This approach extends previous one-dimensional analyses to two spatial dimensions and connects symmetry structure to physically observable wave regimes.

In this study, we perform a Lie group analysis and obtain several classes of symmetry reductions. We find exact travelling wave solutions and analyse their stability for equation (3). We also discuss the physical interpretation of the solutions using graphs based on the results of the stability analysis. Notably, we study the stability of solutions of the travelling wave type, i.e. the stability of wave shape and propagation. The central goal of this study is to analyse Lie groups and explore the resulting solutions for the invariant equation using wave transformations. Specific cases of the nonlinear Klein–Gordon equation related to the Schrödinger equation are considered, with solutions in various forms of travelling waves.

These waves are characterised by their ability to transfer energy. Their intensity characteristics are represented by the square of the wave function's amplitude, simulating the phenomenon of nonlinear dispersion [29].

Consequently, we investigate explicit solutions of the two-dimensional Klein–Gordon equation (3) relevant to plasma physics. The article is structured as follows: In Sect. 2, we employ Lie symmetry analysis for symmetry reductions of

the equation. In Sect. 3, we obtain travelling wave solutions using the conventional $(1/G')$-expansion method. In Sect. 4, we analyse the stability of these travelling wave solutions. In Sect. 5, we illustrate the solution dynamics with 2D and contour plots for suitable parameter values.

2 Lie symmetry method

2.1 Lie symmetry analysis for partial differential equations

Lie symmetry analysis is among the most powerful methods for finding solutions and investigating the symmetry properties of differential equations. This approach, developed by Sophus Lie over a century ago, was further studied by Ovsyannikov, Ibragimov, Olver, and other prominent researchers [30–32]. The method provides a systematic approach to constructing invariant equations by reducing the dimensionality of the differential equation. Many researchers have explored symmetry groups in numerous papers and books [22, 33, 34].

In this section, we present a general overview of Lie symmetry analysis for partial differential equations (PDEs) of the form:

$$F(t, x, y, u, v, u_t, v_t, u_x, u_y, v_x, v_y, u_{xx}, u_{yy}, v_{xx}, v_{yy}) = 0. \tag{4}$$

A one-parameter Lie symmetry transformation, which acts on the space of three independent variables (t, x, y) and two dependent variables u and v, is defined as follows:

$$\begin{aligned}
\bar{t} &= t + \varepsilon\tau(t, x, y, u, v) + O(\varepsilon^2),\\
\bar{x} &= x + \varepsilon\xi_1(t, x, y, u, v) + O(\varepsilon^2),\\
\bar{y} &= y + \varepsilon\xi_2(t, x, y, u, v) + O(\varepsilon^2),\\
\bar{u} &= u + \varepsilon\eta_1(t, x, y, u, v) + O(\varepsilon^2),\\
\bar{v} &= v + \varepsilon\eta_2(t, x, y, u, v) + O(\varepsilon^2),
\end{aligned} \tag{5}$$

where $\varepsilon > 0$ is an infinitesimal group parameter. The corresponding infinitesimal generator, associated with the above transformation, is given by:

$$\begin{aligned}
X = {} & \xi_1(t, x, y, u, v)\frac{\partial}{\partial x} + \xi_2(t, x, y, u, v)\frac{\partial}{\partial y}\\
& + \tau(t, x, y, u, v)\frac{\partial}{\partial t}\\
& + \eta_1(t, x, y, u, v)\frac{\partial}{\partial u} + \eta_2(t, x, y, u, v)\frac{\partial}{\partial v}.
\end{aligned} \tag{6}$$

According to the infinitesimal transformation (5), the second-order prolongation pr^2X of the generator X for the PDE (4) takes the form:

$$\begin{aligned}
pr^2X = {} & X + \eta_1^t\partial_{u_t} + \eta_2^t\partial_{v_t} + \eta_1^{tt}\partial_{u_{tt}} + \eta_2^{tt}\partial_{v_{tt}} + \eta_1^x\partial_{u_x}\\
& + \eta_1^y\partial_{u_y} + \eta_2^x\partial_{v_x} + \eta_2^y\partial_{v_y} + \eta_1^{xx}\partial_{u_{xx}}\\
& + \eta_1^{yy}\partial_{u_{yy}} + \eta_2^{xx}\partial_{v_{xx}} + \eta_2^{yy}\partial_{v_{yy}},
\end{aligned} \tag{7}$$

where the coefficients η are defined as:

$$\begin{aligned}
\eta_1^t &= D_t\eta_1 - u_xD_t\xi_1 - u_yD_t\xi_2 - u_tD_t\tau,\\
\eta_2^t &= D_t\eta_2 - v_xD_t\xi_1 - v_yD_t\xi_2 - v_tD_t\tau,\\
\eta_1^{tt} &= D_t\eta_1^t - u_{tx}D_t\xi_1 - u_{ty}D_t\xi_2 - u_{tt}D_t\tau,\\
\eta_2^{tt} &= D_t\eta_2^t - v_{tx}D_t\xi_1 - v_{ty}D_t\xi_2 - v_{tt}D_t\tau,\\
\eta_1^x &= D_x\eta_1 - u_xD_x\xi_1 - u_yD_x\xi_2 - u_tD_x\tau,\\
\eta_2^x &= D_x\eta_2 - v_xD_x\xi_1 - v_yD_x\xi_2 - v_tD_x\tau,\\
\eta_1^y &= D_y\eta_1 - u_xD_y\xi_1 - u_yD_y\xi_2 - u_tD_y\tau,\\
\eta_2^y &= D_y\eta_2 - v_xD_y\xi_1 - v_yD_y\xi_2 - v_tD_y\tau,\\
\eta_1^{xx} &= D_x\eta_1^x - u_{xx}D_x\xi_1 - u_{xy}D_x\xi_2 - u_{xt}D_x\tau,\\
\eta_2^{xx} &= D_x\eta_2^x - v_{xx}D_x\xi_1 - v_{xy}D_x\xi_2 - v_{xt}D_x\tau,\\
\eta_1^{yy} &= D_y\eta_1^x - u_{yx}D_y\xi_1 - u_{yy}D_y\xi_2 - u_{yt}D_y\tau,\\
\eta_2^{yy} &= D_y\eta_2^x - v_{yx}D_y\xi_1 - v_{yy}D_y\xi_2 - v_{yt}D_y\tau,
\end{aligned}$$

with the total derivative D_i defined as:

$$\begin{aligned}
D_i = {} & \frac{\partial}{\partial i} + u_i\frac{\partial}{\partial u} + v_i\frac{\partial}{\partial v} + u_{ij}\frac{\partial}{\partial u_j} + v_{ij}\frac{\partial}{\partial v_j}\\
& + u_{ii}\frac{\partial}{\partial u_i} + v_{ii}\frac{\partial}{\partial v_i} + \ldots.
\end{aligned}$$

2.2 Lie group analysis of the p-defocusing Klein–Gordon equation

We begin by representing the complex-valued solution of the equation (3) in terms of its real and imaginary parts,

$$q(t, x, y) = u(t, x, y) + iv(t, x, y),$$

where u and v are real-valued functions. Substitution into the equation (3) and separation of real and imaginary parts yields the coupled system:

$$\begin{cases}
v\left(1 + (u^2 + v^2)^{\frac{p-1}{2}}\right) + v_{tt} - v_{xx} - v_{yy} = 0,\\
u\left(1 + (u^2 + v^2)^{\frac{p-1}{2}}\right) + u_{tt} - u_{xx} - u_{yy} = 0,
\end{cases} \tag{8}$$

which will be the object of the subsequent Lie symmetry analysis.

2.2.1 Infinitesimal transformations and prolongation

We consider a one-parameter Lie group of point transformations (5) generated infinitesimally by the vector field (6).

Since system (8) involves second-order derivatives, we require the second prolongation $\mathrm{pr}^2 X$, given by (7) where the extended infinitesimals are computed using the standard prolongation formulas (see, e.g. [31]).

2.2.2 Invariance condition and determining equations

System (8) is invariant under the transformation generated by X if and only if

$$\mathrm{pr}^2 X(F_i)\big|_{F_1=0,\,F_2=0} = 0, \qquad i = 1, 2,$$

where

$$F_1 = v\left(1 + (u^2+v^2)^{\frac{p-1}{2}}\right) + v_{tt} - v_{xx} - v_{yy},$$
$$F_2 = u\left(1 + (u^2+v^2)^{\frac{p-1}{2}}\right) + u_{tt} - u_{xx} - u_{yy}.$$

For brevity, we introduce $R = u^2+v^2$. Applying $\mathrm{pr}^2 X$ and eliminating second-order derivatives using system (8), we obtain a polynomial expression in the independent derivatives and powers of u and v after collecting terms. Setting the coefficients of all functionally independent terms to zero yields an overdetermined system of linear partial differential equations for the infinitesimals, known as the determining equations.

2.2.3 Restriction to point and geometric symmetries

We restrict attention to point symmetries,

$$\xi_1 = \xi_1(t,x,y), \quad \xi_2 = \xi_2(t,x,y), \quad \tau = \tau(t,x,y),$$

$$\eta_1 = \eta_1(t,x,y,u,v), \quad \eta_2 = \eta_2(t,x,y,u,v),$$

which is physically justified by the homogeneous structure of the Klein–Gordon equation.

2.2.4 Solution of the determining equations

Solving the determining equations yields the following results.

Independent variables. From the coefficients of the second-order derivatives,

$$\tau_t = 0, \qquad \xi_{1,x} = 0, \qquad \xi_{2,y} = 0, \qquad \xi_{1,y} + \xi_{2,x} = 0.$$

These equations imply

$$\tau = c_5 x + c_6 y + c_3,$$
$$\xi_1 = c_5 t + c_4 y + c_1,$$
$$\xi_2 = c_6 t - c_4 x + c_2,$$

where $c_1, \ldots, c_6$ are arbitrary constants.

Dependent variables. The determining equations for η_1 and η_2 admit the solution

$$\eta_1 = c_7 v, \qquad \eta_2 = -c_7 u,$$

which corresponds to invariance under global phase rotations $q \mapsto e^{i\theta} q$.

All remaining determining equations are identically satisfied.

2.2.5 Basis of infinitesimal generators

The Lie algebra of point symmetries of system (8) is spanned by the seven generators

$$X_1 = \partial_x, \qquad X_2 = \partial_y, \qquad X_3 = \partial_t,$$
$$X_4 = y\partial_x - x\partial_y,$$
$$X_5 = x\partial_t + t\partial_x, \qquad X_6 = y\partial_t + t\partial_y,$$
$$X_7 = v\partial_u - u\partial_v.$$

These generators correspond, respectively, to translations in space and time, rotations in the (x, y)-plane, Galilean boosts, and global phase rotations.

These symmetry operators form a Lie algebra, and commutation relations $[X_i, X_j] = X_i X_j - X_j X_i$, $(i, j = 1, \ldots, 7)$ define the Lie algebra structure summarised in the next table:

Table 1 Commutation relations of the Lie algebra

	X_1	X_2	X_3	X_4	X_5	X_6	X_7
X_1	0	0	0	$-X_2$	X_3	0	0
X_2		0	0	X_1	0	X_3	0
X_3			0	0	X_1	X_2	0
X_4				0	X_6	$-X_5$	0
X_5					0	$-X_4$	0
X_6						0	0
X_7							0

The commutation relations in Table 1 give the following:

- X_1, X_2, and X_3 generate an abelian translation subalgebra;

- X_4 generates spatial rotations and does not commute with X_1 and X_2;
- X_5 and X_6 represent Galilean boosts;
- X_7 generates the $U(1)$ phase symmetry intrinsic to the complex formulation.

This completes the classification of Lie point symmetries admitted by the p-defocusing Klein–Gordon equation. We have identified all point symmetries through a systematic analysis of the determining equations. The absence of additional dynamical symmetries can be verified by considering the structure of the nonlinearity $|q|^{p-1}q$.

2.3 Symmetry reductions and invariant solutions

Having determined the Lie point symmetry generators $X_1, \ldots, X_7$ in the previous section, we now demonstrate how these symmetries lead systematically to symmetry reductions and invariant solutions of the governing system. In contrast to ad hoc ansatz-based approaches, the Lie symmetry method guarantees that the reduced equations inherit the invariance properties of the original system. This provides a mathematically consistent and exhaustive framework for the construction of exact and physically meaningful solutions.

Let $X_1, \ldots, X_7$ be the Lie point symmetries obtained in Sect. 2.2. A fundamental consequence of Lie invariance is the possibility of reducing the number of independent variables and constructing exact invariant solutions.

A solution

$$q(t, x, y) = u(t, x, y) + iv(t, x, y)$$

is said to be invariant under a symmetry generator

$$X = \xi_1 \partial_x + \xi_2 \partial_y + \tau \partial_t + \eta_1 \partial_u + \eta_2 \partial_v$$

if it satisfies the invariance conditions

$$X[u] = 0, \qquad X[v] = 0.$$

Invariant solutions are obtained by solving the characteristic (Lagrange–Charpit) system

$$\frac{dt}{\tau} = \frac{dx}{\xi_1} = \frac{dy}{\xi_2} = \frac{du}{\eta_1} = \frac{dv}{\eta_2},$$

whose integrals determine the invariant variables and the functional form of the solution. Substitution into the original system then yields a reduced equation of lower dimension. Solving this system yields the invariants of X and thus determines the symmetry-reduced variables.

Case 1: Translation Symmetries X_1 ***and*** X_2.

We consider the one-parameter family of translation generators

$$X = X_1 + k_1 X_2 = \partial_x + k_1 \partial_y, \qquad k_1 \in \mathbb{R}.$$

The characteristic equations reduce to

$$\frac{dx}{1} = \frac{dy}{k_1}, \qquad dt = du = dv = 0,$$

which yield the invariant variable

$$z = x + k_1 y.$$

Accordingly, invariant solutions take the form

$$u(t, x, y) = U(t, z), \qquad v(t, x, y) = V(t, z).$$

Under this transformation, the Laplacian becomes

$$\Delta = (1 + k_1^2)\partial_{zz},$$

and system (8) reduces to

$$\begin{cases} V\left(1 + (U^2 + V^2)^{\frac{p-1}{2}}\right) + V_{tt} - (1 + k_1^2)V_{zz} = 0, \\ U\left(1 + (U^2 + V^2)^{\frac{p-1}{2}}\right) + U_{tt} - (1 + k_1^2)U_{zz} = 0. \end{cases} \tag{9}$$

Case 2: Galilean-Type Symmetry $X_5 + k_2 X_6$.

We next consider the Galilean combination

$$X = X_5 + k_2 X_6, \qquad k_2 \in \mathbb{R}.$$

Solving the characteristic equations yields the quadratic invariant ζ, given by

$$\zeta = (1 + k_2^2)t^2 - (x + k_2 y)^2,$$

and invariant solutions of the form

$$u(t, x, y) = W(\zeta), \qquad v(t, x, y) = S(\zeta).$$

Substitution into system (8) leads to the reduced system of ordinary differential equations

$$\begin{cases} S\left(1 + (W^2 + S^2)^{\frac{p-1}{2}}\right) + 4(1 + k_2^2)(S' + \zeta S'') = 0, \\ W\left(1 + (W^2 + S^2)^{\frac{p-1}{2}}\right) + 4(1 + k_2^2)(W' + \zeta W'') = 0. \end{cases}$$

Case 3: Rotational Symmetry X_4.

Consider the rotational generator

$$X_4 = y\partial_x - x\partial_y.$$

The characteristic equations imply the invariant

$$\zeta = x^2 + y^2,$$

while t remains an independent variable. Hence, invariant solutions are of the form:

$$u(t, x, y) = Q(t, \zeta), \qquad v(t, x, y) = R(t, \zeta).$$

Using

$$\Delta = 4\partial_\zeta + 4\zeta\,\partial_{\zeta\zeta},$$

system (8) reduces to

$$\begin{cases} R\left(1 + (Q^2 + R^2)^{\frac{p-1}{2}}\right) + R_{tt} - 4R_\zeta - 4\zeta R_{\zeta\zeta} = 0, \\ Q\left(1 + (Q^2 + R^2)^{\frac{p-1}{2}}\right) + Q_{tt} - 4Q_\zeta - 4\zeta Q_{\zeta\zeta} = 0. \end{cases}$$

Case 4: Phase Rotation Symmetry X_7.

The generator

$$X_7 = v\partial_u - u\partial_v$$

corresponds to global phase invariance. The characteristic equations yield the invariant

$$u^2 + v^2 = \text{const}.$$

Restricting to invariant solution subspaces associated with the phase symmetry, we impose

$$u = \pm v,$$

which reduces system (8) to the scalar equation

$$u_{tt} - u_{xx} - u_{yy} + u\left(1 + 2^{\frac{p-1}{2}} u^{p-1}\right) = 0.$$

Case 5: Travelling wave reductions via combined symmetries $X_1 + k_1 X_2 + cX_3$.

Travelling wave solutions arise from the combined symmetry

$$X = X_1 + k_1 X_2 + cX_3,$$

where c is the wave speed. The characteristic equations yield the invariant variable

$$v = ct + x + k_1 y.$$

Invariant solutions take the form

$$u = U(v), \qquad v = V(v).$$

Substitution into system (8) leads to

$$\begin{cases} V\left(1 + (U^2 + V^2)^{\frac{p-1}{2}}\right) + (c^2 - 1 - k_1^2)V'' = 0, \\ U\left(1 + (U^2 + V^2)^{\frac{p-1}{2}}\right) + (c^2 - 1 - k_1^2)U'' = 0. \end{cases}$$

Exploiting the internal phase symmetry of the system, we restrict ourselves to invariant solution subspaces defined by $U = \pm V$.

$$(c^2 - 1 - k_1^2)V'' + V + 2^{(p-1)/2} V^p = 0 \tag{10}$$

The reductions presented above demonstrate that all invariant variables and reduced equations arise as direct consequences of the Lie symmetry structure of the p-defocusing Klein–Gordon equation.

The Lie group method, therefore, provides a systematic and complete framework for constructing exact solutions, rather than relying on ad hoc ansätze.

Next, we will attempt to solve certain specific forms of the system (3).

3 Exact solutions of the p-defocusing Klein–Gordon equation

In this section, we study the travelling wave solutions to the p-defocusing Klein–Gordon equation (3). We employ the classical method of separation of variables [35] as well as the $(1/G')$-expansion method [29, 39].

For instance, by combining the symmetry operators X_1 and X_2, we derive a new system (9), which can be reduced to an ordinary differential equation by applying the travelling wave transformation $ct + z$. This transformation leads to travelling wave solutions, which play an important role in fibre optics and wave propagation theory. There are various robust and efficient methods for finding solutions to nonlinear partial differential equations in the form of travelling waves, such as the generalised Kudryashov method [36], the Exp-function method [37, 38], and the homogeneous balance method, among others. In this study, we utilise the $(1/G')$-expansion method [29, 39]. Additionally, we apply the method of separation of variables by decomposing the equation into temporal and spatial components.

3.1 Analysis of the (1/G')-expansion method

In this section, we present the main steps of the $(1/G')$-expansion method for finding travelling wave solutions for a system of nonlinear partial differential equations (PDEs).

Consider the following nonlinear system of evolution equations:

$$Q(w, v, w_t, v_t, w_x, v_x, w_y, v_y, w_{tt}, v_{tt}, \ldots) = 0, \tag{11}$$

where Q is a polynomial in $w(t, x, y)$, $v(t, x, y)$ and their partial derivatives, which includes the highest-order derivatives and nonlinear terms. Under the travelling wave transformation $w(t, x, y) = W(\nu)$, $v(t, x, y) = V(\nu)$, where $\nu = ct + x + k_{1y}$, the above equation can be reduced to the following system of nonlinear ordinary differential equations (ODEs):

$$P(W, V, W', V', W'', V'', \ldots) = 0, \tag{12}$$

where P is a polynomial in $W(\nu)$, $V(\nu)$, and their derivatives with respect to ν.

We assume that the solution of equation (12) can be expressed as a polynomial in $1/G'(\nu)$ as follows:

$$W(\nu) = \sum_{j=0}^{M} a_j \left(\frac{1}{G'(\nu)}\right)^j, \quad V(\nu) = \sum_{j=0}^{M} b_j \left(\frac{1}{G'(\nu)}\right)^j, \tag{13}$$

where M is the homogeneous balance number determined by the highest-order derivatives and nonlinear terms. The function $G(\nu)$ satisfies the following second-order linear ODE:

$$G''(\nu) + \lambda G'(\nu) + \mu = 0, \tag{14}$$

where a_j and b_j $(j = 1, 2, \ldots, M)$, along with the constants λ and μ, are real numbers that will be determined later. The solution to the ODE (14) is given by:

$$G(\nu) = -\frac{\mu\nu}{\lambda} + Se^{-\lambda\nu} + T,$$

where S and T are integration constants. Thus, $\frac{1}{G'(\nu)}$ can be expressed as:

$$\frac{1}{G'(\nu)} = \frac{\lambda}{-\mu + \lambda S\cosh(\lambda\nu) - \lambda S\sinh(\lambda\nu)}.$$

By substituting equation (13) into equation (12) and using equation (14), we obtain a polynomial in terms of $1/G'(\nu)$. By collecting all terms with powers of $1/G'(\nu)$ and setting the coefficients of each power to zero, we derive a system of algebraic equations. Solving this system yields the unknown coefficients a_j and b_j $(j = 1, 2, \ldots, M)$, as well as the constants λ and μ, which allows us to construct the exact solutions to equation (11).

3.2 Applying the (1/G′)-expansion method to obtain exact solutions

In this section, we apply the $(1/G')$-expansion method to derive solutions for the system (10). We will consider the cases when $p = 2$ and $p = 3$. When $p = 2$, equation (10) simplifies to:

$$(c^2 - 1 - k_1^2)V'' + V + 2^{\frac{1}{2}}V^2 = 0$$

Following the steps of the $(1/G')$-expansion method, we define the homogeneous balance number as $M = 2$. This leads to the following algebraic system:

$$\begin{aligned}
&\left(\frac{1}{G'(\nu)}\right)^0 : \sqrt{2}a_0^2 + a_0 = 0,\\
&\left(\frac{1}{G'(\nu)}\right)^1 : a_1c^2\lambda^2 - a_1k_1^2\lambda^2 - a_1\lambda^2 + 2\sqrt{2}a_0a_1 + a_1 = 0,\\
&\left(\frac{1}{G'(\nu)}\right)^2 : 4a_2c^2\lambda^2 + 3a_1c^2\lambda\mu - 4a_2k_1^2\lambda^2 - 3a_1k_1^2\lambda\mu\\
&\quad - 4a_2\lambda^2 - 3a_1\lambda\mu + \sqrt{2}a_1^2 + 2\sqrt{2}a_0a_2 + a_2 = 0,\\
&\left(\frac{1}{G'(\nu)}\right)^3 : 10a_2c^2\lambda\mu + 2a_1c^2\mu^2 - 10a_2k_1^2\lambda\mu\\
&\quad - 2a_1k_1^2\mu^2 - 10a_2\lambda\mu - 2a_1\mu^2 + 2\sqrt{2}a_1a_2 = 0,\\
&\left(\frac{1}{G'(\nu)}\right)^4 : 6a_2c^2\mu^2 - 6a_2k_1^2\mu^2 - 6a_2\mu^2 + \sqrt{2}a_2^2 = 0.
\end{aligned}$$

By solving this system, we obtain the coefficients a_0, a_1, and a_2, as well as the parameters λ and μ. The solutions can be written as: Substituting the obtained coefficients with upper and lower signs into the equation (13) and taking into account the expression $\frac{1}{G'}$, we have, respectively, the following solutions:

$$\begin{aligned}
&a_0 = -\tfrac{1}{\sqrt{2}}, \quad a_1 = \frac{\frac{6c^2\mu}{\sqrt{c^2-k_1^2-1}} - \frac{6k_1^2\mu}{\sqrt{c^2-k_1^2-1}} - \frac{6\mu}{\sqrt{c^2-k_1^2-1}}}{\sqrt{2}},\\
&a_2 = -3\sqrt{2}\mu^2(c^2 - k_1^2 - 1), \quad \lambda = -\frac{1}{\sqrt{c^2-k_1^2-1}}.
\end{aligned}$$

Substituting these coefficients into the solution form (13), taking into account the expression $\frac{1}{G'}$, we have, respectively, the following solutions:

$$q_2(t,x,y)=\left[\frac{\frac{6c^2\mu}{\sqrt{-c^2+k_1^2+1}}-\frac{6k_1^2\mu}{\sqrt{-c^2+k_1^2+1}}-\frac{6\mu}{\sqrt{-c^2+k_1^2+1}}}{\sqrt{2}\left(C_1\left(\sinh\frac{ct+x+k_1y}{\sqrt{-c^2+k_1^2+1}}+\cosh\frac{ct+x+k_1y}{\sqrt{-c^2+k_1^2+1}}\right)+\mu\sqrt{-c^2+k_1^2+1}\right)}\right.$$
$$\left.-\frac{3\sqrt{2}\mu^2\left(c^2-k_1^2-1\right)}{\left(C_1\left(\sinh\frac{ct+x+k_1y}{\sqrt{-c^2+k_1^2+1}}+\cosh\frac{ct+x+k_1y}{\sqrt{-c^2+k_1^2+1}}\right)+\mu\sqrt{-c^2+k_1^2+1}\right)^2}\right](1\pm i).$$

$$q_1(t,x,y)=\left[-\frac{3\sqrt{2}\mu^2(c^2-k_1^2-1)}{\left(C_1\sinh\frac{ct+x+k_1y}{\sqrt{c^2-k_1^2-1}}+\cosh\frac{ct+x+k_1y}{\sqrt{c^2-k_1^2-1}}\right)^2}\right.$$
$$\left.+\frac{a_1}{C_1\sinh\left(\frac{ct+x+k_1y}{\sqrt{c^2-k_1^2-1}}\right)+\mu\sqrt{c^2-k_1^2-1}}\right](1\pm i). \quad (15)$$

On the other hand, we have the next case:

$$a_0=0,\ a_1=\frac{\frac{6c^2\mu}{\sqrt{-c^2+k_1^2+1}}-\frac{6k_1^2\mu}{\sqrt{-c^2+k_1^2+1}}-\frac{6\mu}{\sqrt{-c^2+k_1^2+1}}}{\sqrt{2}},$$

$$a_2=-3\sqrt{2}\mu^2\left(c^2-k_1^2-1\right),\ \lambda=-\frac{1}{\sqrt{-c^2+k_1^2+1}}$$

which gives

The resulting solutions are travelling wavefront with $\sqrt{1+k_1^2}$ is the wave number, c is the wave speed, and $c/\sqrt{1+k_1^2}$ is the phase velocity of the travelling wave, respectively, and singular solutions that will be discussed in the following sections.

Now let's consider the case $p=3$. Here the equation (10) takes a form:

$$(c^2-1-k_1^2)V''+V+2V^3=0$$

We define the homogeneous balance number as $M=1$, leading to the following algebraic system:

$$\left(\frac{1}{G'(\nu)}\right)^0: 2a_0^3+a_0=0,$$
$$\left(\frac{1}{G'(\nu)}\right)^1: a_1(-c^2\lambda^2+k_1^2\lambda^2+\lambda^2)-6a_0^2a_1-a_1=0,$$
$$\left(\frac{1}{G'(\nu)}\right)^2: -3a_1c^2\lambda\mu+3a_1k_1^2\lambda\mu+3a_1\lambda\mu+6a_0a_1^2=0,$$
$$\left(\frac{1}{G'(\nu)}\right)^3: -2a_1c^2\mu^2+2a_1k_1^2\mu^2+2a_1\mu^2-2a_1^3=0.$$

The solution for this system yields:

$$a_0=-\frac{i}{\sqrt{2}},\quad a_1=-i\left(\frac{c^2\mu}{\sqrt{c^2-k_1^2-1}}-\frac{k_1^2\mu}{\sqrt{c^2-k_1^2-1}}-\frac{\mu}{\sqrt{c^2-k_1^2-1}}\right),$$
$$\lambda=-\frac{\sqrt{2}}{\sqrt{c^2-k_1^2-1}}.$$

The resulting solution to the equation (3) for $p=3$ is:

$$q_3(t,x,y)=\left[\frac{\frac{c^2\mu}{\sqrt{c^2-k_1^2-1}}-\frac{k_1^2\mu}{\sqrt{c^2-k_1^2-1}}-\frac{\mu}{\sqrt{c^2-k_1^2-1}}}{C_1\left(\sinh\frac{\sqrt{2}(ct+x+k_1y)}{\sqrt{c^2-k_1^2-1}}+\cosh\frac{\sqrt{2}(ct+x+k_1y)}{\sqrt{c^2-k_1^2-1}}\right)+\frac{\mu\sqrt{c^2-k_1^2-1}}{\sqrt{2}}}-\frac{1}{\sqrt{2}}\right](i\pm 1) \quad (16)$$

When $p \neq 2$ and $p \neq 3$ the homogeneous balance number is defined as $M = \frac{2}{p-1}$, which will not be an integer. This situation leads to more complex cases.

We verified the correctness of solutions (15) and (16) by direct substitution into the original equation (3). The algebraic computations were performed using Wolfram Mathematica 13, confirming that both solutions satisfy the p-defocusing Klein–Gordon equation identically for the obtained parameter relations.

Having obtained exact solutions for the cases $p = 2$ and $p = 3$, we now turn to analysing their stability properties through linear perturbation theory.

4 Linear stability analysis of uniform background states

Before analysing the stability of the travelling wave solutions obtained in Sect. 3, we first examine the simpler problem of linear stability of spatially uniform (constant) background states. This preliminary analysis establishes the baseline dispersion relation and identifies parameter regimes where the uniform state is susceptible to instabilities.

We consider small perturbations around a spatially uniform background solution $q(t, x, y) \equiv C_0 = \text{const}$. Note that for equation (3), uniform states satisfy $C_0(1 + |C_0|^{p-1}) = 0$, which yields either $C_0 = 0$ or $|C_0|^{p-1} = -1$. For real C_0 and $p > 1$, only $C_0 = 0$ is admissible; however, complex uniform states exist (e.g. $C_0 = \pm i/\sqrt{3}$ for $p = 3$).

The stability of such uniform states is examined by considering perturbed solutions of the form

$$q(t, x, y) = C_0 + \sigma W(t, x, y), \tag{17}$$

where $\sigma \ll 1$ is a small parameter.

Substituting (17) into equation (3), expanding to first order in σ, and noting that C_0 satisfies $C_0(1 + |C_0|^{p-1}) = 0$, we obtain the linearised equation for the perturbation:

$$W_{tt} - W_{xx} - W_{yy} + W(1 + pC_0^{p-1}) = 0. \tag{18}$$

This is a linear constant-coefficient PDE. We seek plane wave solutions of the form

$$W(t, x, y) = e^{i(k(x+y)-mt)}, \quad \text{or} \quad W(t, x, y) = e^{ik(x+y)-\varrho t}, \tag{19}$$

where k is the wave number, m is the frequency of perturbation, m/k is the wave's phase velocity, and ϱ, depending on its sign, indicates the growth or decay of the perturbation. The first form describes oscillatory behaviour, while the second form is used to study exponential growth or decay. A negative real part of ϱ corresponds to damping, a positive real part to growth, and $\mathrm{Re}(\varrho) = 0$ to marginal (neutral) stability, where perturbations oscillate with constant amplitude.

Substituting into the linearised equation yields the dispersion relation:

$$m = \pm\sqrt{2k^2 + 1 + pC_0^{p-1}}. \tag{20}$$

This characterises the evolution of linear perturbations superimposed on the uniform background C_0.

For the case $2k^2 + 1 + pC_0^{p-1} > 0$, the frequency m is real for all real k, implying that perturbations oscillate without exponential growth or decay—a signature of *marginal stability* characteristic of conservative Hamiltonian systems. In this regime, the uniform state C_0 is *linearly stable* against small perturbations, although nonlinear effects (not captured by this analysis) may lead to long-term instabilities.

However, if $2k^2 + 1 + pC_0^{p-1} < 0$ for some range of k, then m becomes imaginary, indicating that ϱ acquires a nonzero real part and perturbations grow exponentially—the uniform state is *unstable*.

From the dispersion relation, we obtain the phase velocity

$$\frac{m}{k} = \pm\frac{\sqrt{2k^2 + 1 + pC_0^{p-1}}}{k}, \tag{21}$$

which gives the velocity of wave fronts, and the group velocity

$$\frac{dm}{dk} = \pm\frac{2k}{\sqrt{2k^2 + 1 + pC_0^{p-1}}}, \tag{22}$$

which gives the velocity of wave packets.

The growth rate is given by

$$\varrho = \pm\sqrt{-2k^2 - 1 - pC_0^{p-1}} = \pm i\sqrt{2k^2 + 1 + pC_0^{p-1}}. \tag{23}$$

When $C_0^{p-1} > \frac{-(1+2k^2)}{p}$, ϱ is purely imaginary, corresponding to oscillatory (non-growing) perturbations—marginal stability. Conversely, if $C_0^{p-1} < \frac{-(1+2k^2)}{p}$ for some k, ϱ acquires a nonzero real part, leading to exponential instability.

For the specific case $p = 3$, the stability condition becomes $C_0^2 > \frac{-(1+2k^2)}{3}$.

Case 1: Real uniform background ($C_0 \in \mathbb{R}$).

Since $C_0^2 \geq 0$ and $\frac{-(1+2k^2)}{3} < 0$ for all k, the condition is always satisfied. Thus, any real uniform background is marginally stable—small perturbations oscillate without growth.

Case 2: Complex uniform background ($C_0 = ia, a \in \mathbb{R}$).

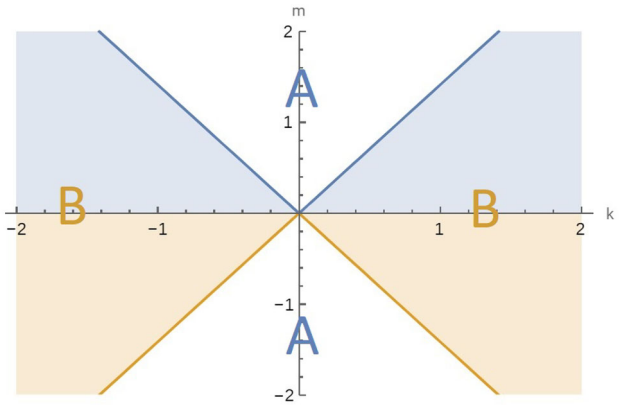


Fig. 1 Stability diagram for the uniform background state $C_0 = \pm i/\sqrt{3}$ with $p = 3$. The curves $m = \pm\sqrt{2k^2 + 1 + 3C_0^2}$ separate parameter space into regions of different behaviour. **Region A** (shaded): Real m, corresponding to oscillatory perturbations (marginally stable uniform background). **Region B** (unshaded): Imaginary m, corresponding to exponential growth/decay (unstable uniform background). *Note:* This diagram characterises perturbations around a *uniform* state, not the stability of the localised travelling waves derived in Sect. 3

Here $C_0^2 = -a^2 < 0$. The stability condition becomes:

$$-a^2 > \frac{-(1+2k^2)}{3} \quad \Leftrightarrow \quad a^2 < \frac{1+2k^2}{3}. \tag{24}$$

Thus, the uniform state $C_0 = ia$ is:

- *Stable* (marginally) if $a < \sqrt{\frac{1+2k^2}{3}}$ for all k (oscillatory perturbations),
- *Unstable* if $a > \sqrt{\frac{1+2k^2}{3}}$ for some k (exponential growth).

Figure 1 illustrates the stability regions in the (k, m)-plane for the specific choice $C_0 = \pm\frac{i}{\sqrt{3}}$, which lies at the marginal stability boundary for $k = 0$.

The linear stability analysis presented above applies strictly to *spatially uniform background states* $C_0 = \text{const}$. It identifies parameter regimes where such uniform states are susceptible to modulational instabilities, which can seed the formation of localised structures.

However, this analysis does *not* directly address the stability of the *localised travelling wave solutions* q_1, q_2, and q_3 obtained in Sect. 3 via the $(1/G')$-expansion method. The stability of such nontrivial coherent structures requires a different approach, typically involving:

- Linearisation around the *moving wave profile* in a co-moving frame,
- Spectral analysis of the resulting linear operator with non-constant coefficients,
- Numerical computation of eigenvalues/eigenfunctions.

Such analysis lies beyond the scope of the present work. Nevertheless, the qualitative features observed in Sect. 5 (localisation for $c^2 > k_1^2 + 1$, oscillatory structure for $c^2 < k_1^2 + 1$) are consistent with the parameter-dependent behaviour suggested by the dispersion relation.

In the following section, we present detailed graphical visualisations of the travelling wave solutions and discuss their physical interpretation.

5 Discussion of results and graphics

5.1 Mathematical structure of the solutions

The wave function, in which physical properties such as phase, potential, and group velocity make sense, can be assumed in the form of travelling wave solutions to nonlinear partial differential equations. Before examining the graphical results, we must understand the mathematical structure underlying our solutions.

The travelling wave solutions $q_1(t, x, y)$ and $q_2(t, x, y)$, given by equation (15), as well as $q_3(t, x, y)$ from equation (16), can be written in the form

$$q(t, x, y) = A(t, x, y) \cdot e^{i\phi},$$

where $A(t, x, y)$ is a real-valued amplitude function expressed in terms of superpositions of hyperbolic functions sinh and cosh, and $e^{i\phi}$ represents a constant phase factor. Specifically:

For solutions q_1 and q_2: $e^{i\phi} = \frac{1 \pm i}{\sqrt{2}} = e^{\pm i\pi/4}$ (phase $\pm 45°$)

For solution q_3: $e^{i\phi} = \frac{i \pm 1}{\sqrt{2}} = e^{i(\pm\pi/4 + \pi/2)}$ (phase $\pm 45° + 90°$)

This structure immediately implies that the real and imaginary parts are related, by

$$\text{Re}(q) = A(t, x, y)\cos\phi, \qquad \text{Im}(q) = A(t, x, y)\sin\phi.$$

Since $|\cos\phi| = |\sin\phi| = 1/\sqrt{2}$ for all our solutions, we obtain the key observation:

$$|\text{Re}(q)| = |\text{Im}(q)| = \frac{|A(t, x, y)|}{\sqrt{2}}.$$

In other words, the real and imaginary parts have identical spatial profiles—they differ only by a constant phase factor. This is not coincidental; it follows directly from the phase symmetry X_7 identified in Sect. 2.2, which allows arbitrary rotation in the complex plane.

The constant phase factor carries important physical meaning in different contexts. In plasma physics, the phase difference between real and imaginary parts corresponds to

the phase relationship between electric field oscillations and charge density fluctuations in Langmuir waves. In nonlinear optics, it represents the carrier-envelope phase (CEP) of ultrashort optical pulses—a quantity that becomes crucial when pulse durations approach a few optical cycles. In quantum field theory, this phase encodes the global U(1) gauge degree of freedom of the complex scalar field.

Since equation (3) is invariant under global phase rotations $q \to e^{i\theta} q$ (the symmetry X_7), solutions differing only by a constant phase factor are physically equivalent. This means that the modulus $|q|$ captures all the physically meaningful information about energy density and intensity. However, presenting both real and imaginary parts serves important purposes: It verifies the expected structure $q = A \cdot e^{i\phi}$ with constant ϕ, provides pedagogical clarity for readers unfamiliar with complex field solutions, and establishes a baseline for comparison with more general initial conditions where real and imaginary parts may differ in profile.

5.2 Solution regimes and physical behaviour

For $p = 2$, we found two solutions $q_1(t, x, y)$ and $q_2(t, x, y)$, which have the form of superpositions of hyperbolic functions sinh and cosh. These functions describe the behaviour of the wave depending on the speed c, propagation direction k_1, and frequency μ. The solution $q_1(t, x, y)$ can describe a localised soliton-like wave that moves with a constant speed c. The behaviour depends on the ratio $c^2 - k_1^2 - 1$, which determines the type of the solution.

Regime I: Solitary wave (localised) regime

If $c^2 > k_1^2 + 1$, the hyperbolic functions have a real argument, and the solution remains localised. The amplitude $|q|$ decays exponentially away from the wave centre according to

$$|q(t, x, y)| \sim \frac{\text{const}}{e^{|\nu|/\alpha}}, \quad \text{where} \quad \alpha = \frac{1}{\sqrt{c^2 - k_1^2 - 1}} \in \mathbb{R},$$

creating a localized wave packet. These are solitary travelling wavefront solutions (see Figs. 2, 3 and 5).

The critical threshold $c^2 = k_1^2 + 1$ separating the solitary-wave and oscillatory regimes has a clear physical interpretation. In nonlinear optics, it corresponds to the critical propagation velocity for self-trapping—below this threshold, dispersion dominates and the wave fragments into periodic structures. In plasma physics, this threshold is related to the phase velocity of Langmuir waves; when the wave velocity exceeds the critical value, nonlinearity can balance dispersion to form stable envelope solitons.

In plasma physics, such profiles describe envelope solitons—self-trapped Langmuir wave packets that propagate without spreading, as observed in the Klein–Gordon–Zakharov system [6, 8]. In nonlinear optics, these correspond to localised envelope structures in defocusing Kerr media, which manifest as stable intensity dips on a continuous wave background [17]. From a field theory perspective, they represent solitary scalar field configurations that, while resembling kinks, lack topological charge.

The parameter regime $c^2 > k_1^2 + 1$ is consistent with the formation of localised structures. In this regime, the solutions exhibit exponential decay, ensuring finite energy:

$$E = \int |q|^2 dx dy < \infty.$$

Regime II: Oscillatory (wave train) regime

If $c^2 < k_1^2 + 1$, the argument of the hyperbolic functions becomes imaginary, which can lead to an oscillating solution (see Figs. 4 and 6). The hyperbolic functions transform into trigonometric functions via the standard identities

$$\sinh(i\beta\nu) = i\sin(\beta\nu), \qquad \cosh(i\beta\nu) = \cos(\beta\nu),$$

where $\beta = 1/\sqrt{k_1^2 + 1 - c^2} \in \mathbb{R}$. The amplitude consequently oscillates periodically in space:

$$|q(t, x, y)| \sim |\cos(\beta\nu) + \text{phase shifts}|.$$

These periodic structures have rich physical interpretations. In plasma physics, they represent modulated wave trains with spatial periodicity $\ell = 2\pi/\beta$, which are relevant to understanding quasi-periodic plasma oscillations and energy cascades in turbulent regimes. In nonlinear optics, such patterns arise as periodic intensity modulations in planar waveguides or photonic crystals, where the periodicity ℓ is related to the detuning from the critical propagation velocity.

Regime II: Oscillatory (wave train) regime

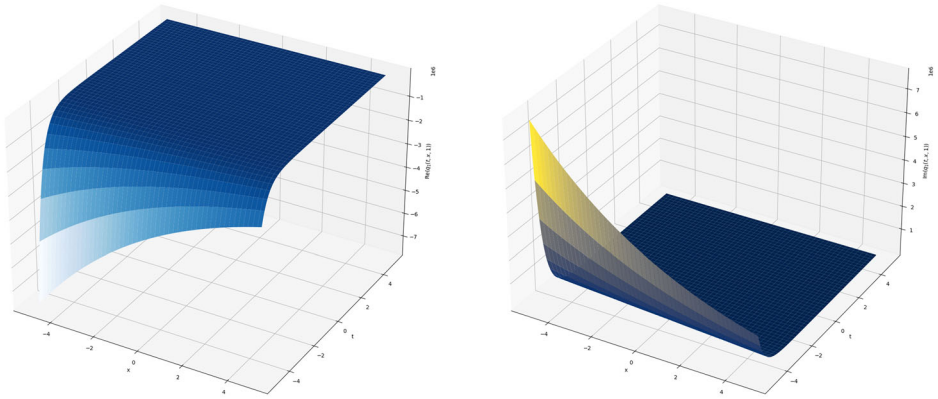
If $c^2 < k_1^2 + 1$, the argument of the hyperbolic functions becomes imaginary, which can lead to an oscillating solution (see Figs. 4 and 6).

The nature of oscillatory solutions depends critically on the nonlinearity parameter p:

- **For** $p = 2$: The hyperbolic functions transform into trigonometric functions via the standard identities

  $$\sinh(i\beta\nu) = i\sin(\beta\nu), \qquad \cosh(i\beta\nu) = \cos(\beta\nu),$$

  where $\beta = 1/\sqrt{k_1^2 + 1 - c^2} \in \mathbb{R}$. This yields a *periodic wave train* extending throughout space—a sequence of waves with spatial periodicity $\ell = 2\pi/\beta$.
  For $p = 3$: The complex-valued parameter λ has both real and imaginary parts, leading to a fundamentally different structure: a modulated localised wave (also termed a spatially localised oscillatory structure). The real part



(a) Real part of the solitary wavefront solution.

(b) Imaginary part of the solitary wavefront solution.

Fig. 2 3D plots of the real and imaginary parts of the solitary travelling wavefront solution (15). Both parts exhibit identical spatial profiles, differing only by the constant phase scaling factor $1/\sqrt{2}$ (see Sect. 5). Parameters: $k_1 = 1$, $\mu = 0.5$, $c = 3$, $C_1 = 1$, $a_1 = 1$, and $y = 1$

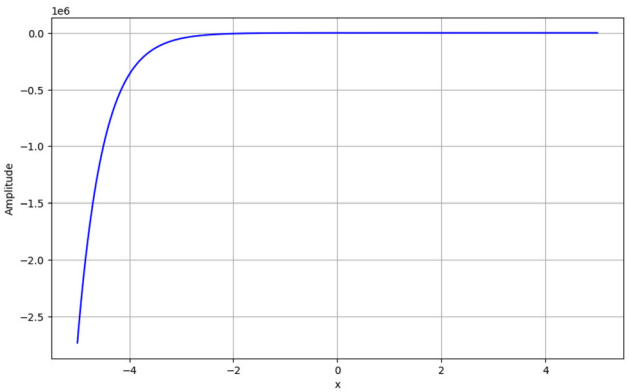


Fig. 3 The cross-section of the solution

of λ produces exponential localisation (an envelope that decays away from the centre), while the imaginary part generates rapid oscillations within this envelope. The result is a single localised wave packet with internal oscillatory structure, rather than an extended periodic pattern.

These periodic structures (for $p = 2$) and spatially modulated localised wave structures (for $p = 3$) have rich physical interpretations:

Periodic wave trains ($p = 2$)**:** In plasma physics, these represent modulated Langmuir oscillations extending throughout space. In nonlinear optics, they correspond to periodic intensity patterns in photonic crystals or planar waveguides. The spatial periodicity $\ell = 2\pi/\beta$ characterises the wavelength of these extended structures.

Modulated localised waves ($p = 3$)**:** These spatially confined oscillatory structures have distinct significance. In plasma physics, they describe self-trapped wave packets with internal modulation while remaining spatially localised—observed in beam–plasma interactions [6, 8]. In nonlinear optics, they represent spatially modulated envelope structures in defocusing media [17], distinct from temporally pulsating spatially modulated localised waves. In field theory, they correspond to oscillon-like configurations or standing-wave envelopes. Unlike the extended wave trains of $p = 2$, these modulated localised waves possess finite energy and combine soliton-like exponential decay with internal periodic oscillations—a signature of higher-order nonlinear effects. The transition from wave trains to modulated localised structures as p increases illustrates how stronger nonlinearities enhance localisation mechanisms while permitting complex internal spatial dynamics.

5.3 Visualisation strategy

Guided by this structure, we adopt a visualisation strategy that emphasises physical transparency while addressing the complex nature of the solutions. The modulus $|q(t, x, y)|$ is presented as the primary quantity, as it is phase-independent and directly related to observable physical measures. For completeness, the real and imaginary parts are also shown separately. Although their profiles coincide in the present case, displaying both components confirms the constant phase structure and provides a useful reference for more general solutions in which the phase may vary spatially.

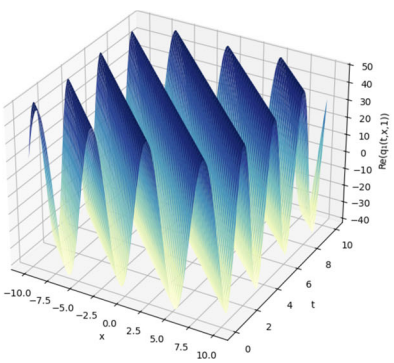
5.4 Graphical results of solution for p = 2

We now present detailed graphical analysis of solution (15), examining representative cases from both parameter regimes.

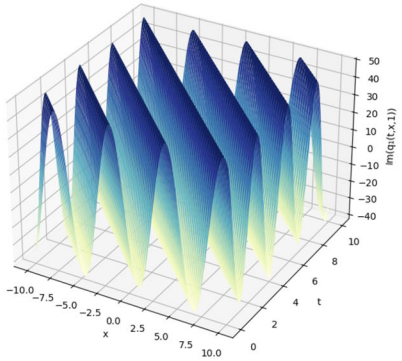
Case A: Solitary wave regime ($c^2 > k_1^2 + 1$)

For this case, we choose parameters $k_1 = 1$, $\mu = 0.5$, $c = 3$, $C_1 = 1$, $a_1 = 1$, and $y = 1$. We can verify that $c^2 - k_1^2 - 1 = 9 - 1 - 1 = 7 > 0$, confirming that we are in Regime I.

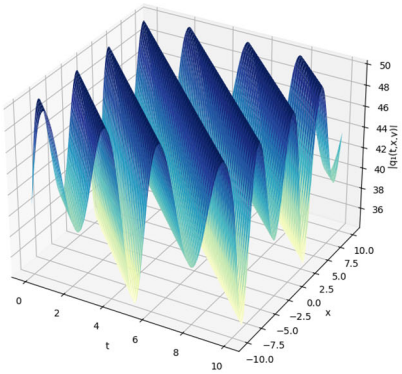
The 3D surface plot in Figure 2a reveals a localised wave packet propagating with constant shape. The amplitude decays exponentially in all directions perpendicular to propagation, with characteristic decay length $\alpha = 1/\sqrt{7} \approx 0.378$.



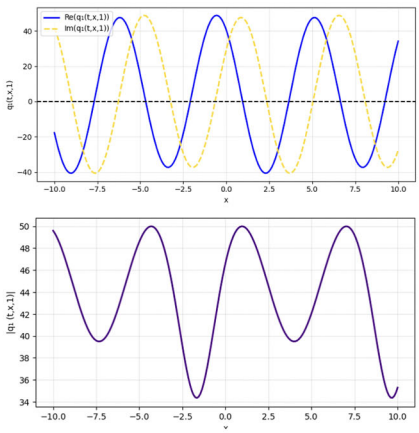
(a) The 3D plot of the real part of the oscillating solution.



(b) The 3D plot of the imaginary part of the oscillating solution.

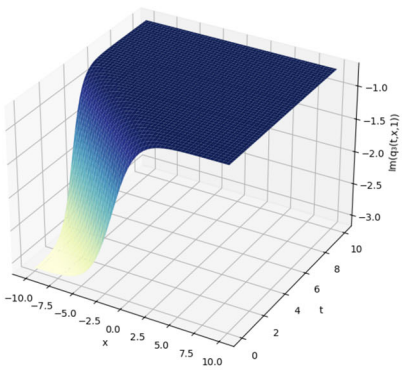


(c) The 3D plot of the absolute of the oscillating solution.

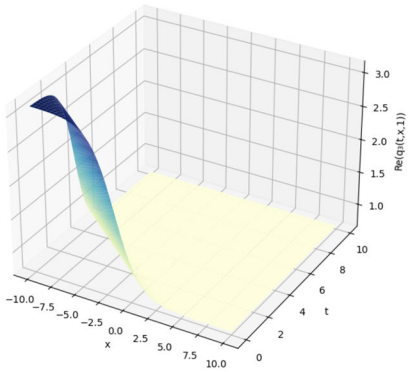


(d) The cross-sections of the oscillating solution and its absolute value.

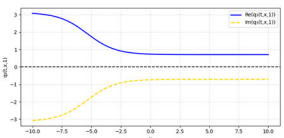
Fig. 4 3D plots and cross-sections of the oscillating solution (15). **a** Real part, **b** imaginary part, **c** absolute value, **d** cross-sections. The real and imaginary parts exhibit identical spatial profiles scaled by the constant phase factor $1/\sqrt{2}$ (see Sect. 5). Parameters: $k_1 = 2.5$, $\mu = 1.5$, $c = 2$, $C_1 = 1$, $a_1 = 1$, and $y = 1$



(a) The 3D plot of the imaginary part of the solitary travelling wavefront solution.

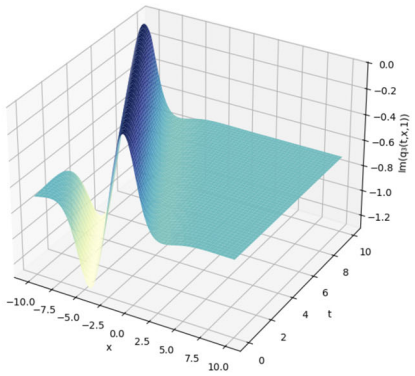


(b) The 3D plot of the real part of the solitary travelling wavefront solution.

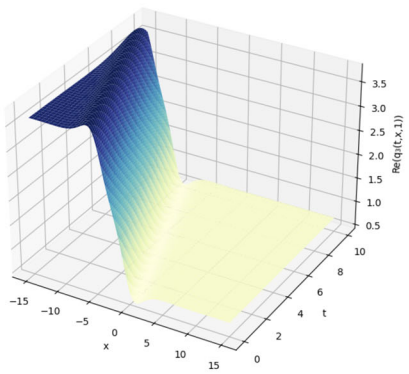


(c) The cross-section of the solitary travelling wavefront solution.

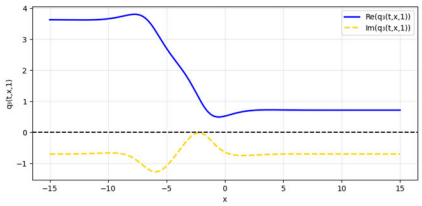
Fig. 5 3D plots of the real part, imaginary part, and the cross-section of the solitary travelling wavefront solution (16). The imaginary part has an identical spatial profile scaled by the constant phase factor (see Sect. 5); thus, only the real part is shown. Parameters: $k_1 = 1$, $\mu = 0.5$, $c = 2.5$, $C_1 = 1$, and $y = 1$



(a) Real part of the modulated localised wave solution.



(b) Imaginary part of the modulated localised wave solution.



(c) Cross-section of the modulated localised wave solution.

Fig. 6 3D plots and cross-section of the modulated localised wave solution (16). **a** Real part shows a spatially localised wave packet with internal oscillatory structure—characteristic of a modulated localised wave formed by complex-valued λ. **b** Imaginary part exhibits an identical spatial profile, scaled by the constant phase factor $1/\sqrt{2}$ (see Sect. 5). **c** Cross-section reveals the exponentially decaying envelope with multiple internal oscillations within the confined region, demonstrating the interplay between localisation ($Re(\lambda)$) and internal modulation ($Im(\lambda)$). Parameters: $k_1 = 1.5$, $\mu = 0.5$, $c = 1$, $C_1 = 1$, and $y = 1$

This localised structure is the hallmark of an envelope soliton.

The imaginary part in Figure 2b exhibits precisely the same spatial structure as the real part, scaled by the phase factor. Depending on the choice of sign in the $\pm i$ factor, it may differ by an overall sign, but the shape is identical. This confirms that the phase factor remains constant across all space—a defining characteristic of travelling wave solutions. Notice that wherever the real part is large, the imaginary part is correspondingly large—the two quantities track each other perfectly in shape.

The two-dimensional cross-section makes the relationships crystal clear. The profile shows exponential decay away from the centre, confirming the solitary-wave nature of the solution. Both real and imaginary parts maintain the same functional form, differing only in their vertical scaling by $1/\sqrt{2}$. All curves peak at the same location and decay at the same rate.

This localised profile represents a stable envelope soliton. In the plasma physics context, it describes a self-trapped Langmuir wave packet where the defocusing nonlinearity precisely balances dispersion, preventing the packet from spreading. The plots of $q_1(t, x, y)$ confirm this, demonstrating stable localisation and shape preservation.

Case B: Oscillatory regime ($c^2 < k_1^2 + 1$)

We now examine the contrasting behaviour in the oscillatory regime, using parameters $k_1 = 2.5$, $\mu = 0.5$, $c = 2$, $C_1 = 1, a_1 = 1$, and $y = 1$. Here $c^2 - k_1^2 - 1 = 4 - 6.25 - 1 = -3.25 < 0$, placing us firmly in Regime II.

In Figure 4 rather than a single localised peak, we now see periodic oscillations in space with a wavelength

$$\ell = \frac{2\pi}{\beta} = 2\pi\sqrt{|c^2 - k_1^2 - 1|} = 2\pi\sqrt{3.25} \approx 11.3.$$

The real part in Figure 4a oscillates with this spatial period and passes through zero at regular intervals, creating nodes where the wave amplitude vanishes. Between these nodes, the amplitude follows a sinusoidal envelope.

The cross-section in Fig. 4d reveals several key features. First, the periodic modulation has wavelength $\ell \approx 11.3$ as predicted. Second, the oscillations maintain regular spacing throughout the domain. The modulus (not shown separately but evident from the profile) provides the "envelope" that bounds the oscillations of the real part.

These periodic solutions represent modulated wave trains or cnoidal-like waves (though expressed through hyperbolic/trigonometric functions rather than Jacobi elliptic functions). In plasma physics, such structures emerge when the wave velocity c falls below the critical threshold, causing the wave to fragment into periodic cells rather than maintaining a localised profile. In nonlinear optics, this regime may correspond to Bloch wave modes in periodic photonic structures, or to filamentation patterns in self-defocusing media.

The solution $q_2(t, x, y)$ is in turn similar to the $q_1(t, x, y)$ solution, but with a different dependence on the parameters. This solution also describes a wave with possible oscillating behaviour, especially depending on the parameters c and k_1.

5.5 Graphical results of solution for p = 3

The solution obtained for the equation at $p = 3$ in the form $q_3(t, x, y)$ has a more complicated form, but also uses hyperbolic functions. The coefficients μ and $c^2 - k_1^2 - 1$ play an important role in the form of the solution.

Case C: Solitary wave regime for $p = 3$

We examine the quintic nonlinearity case with parameters $k_1 = 1$, $\mu = 0.5$, $c = 2.5$, $C_1 = 1$, and $y = 1$. Since $c^2 - k_1^2 - 1 = 6.25 - 1 - 1 = 4.25 > 0$, we remain in the solitary-wave regime.

For $c^2 > k_1^2 + 1$ the hyperbolic functions have a real argument, and q_3 describes a localised wave (see Fig. 5).

The overall structure resembles that of q_1 in Regime I, but with a noticeably different decay rate due to the quintic ($p = 3$) nonlinearity. The characteristic length scale is

$$\alpha = \frac{1}{\sqrt{2(c^2 - k_1^2 - 1)}} = \frac{1}{\sqrt{8.5}} \approx 0.343. \tag{25}$$

The cross-section allows direct comparison with the $p = 2$ case. For comparable values of c and k_1, the $p = 3$ solution exhibits a narrower spatial width—the wave packet decays more rapidly. This reflects the stronger self-defocusing effect associated with higher-order nonlinearities. The solution $q_3(t, x, y)$, which has a more complex structure, was also analysed from the point of view of the dispersion relation. For $c^2 > k_1^2 + 1$, it is stable and preserves the shape of a localised wave, which is visible in the plots.

Case D: Modulated Localised Wave for $p = 3$

Finally, we examine the spatially modulated localised wave regime for $p = 3$ using parameters $k_1 = 1.5$, $\mu = 0.5$, $c = 1$, $C_1 = 1$, and $y = 1$. With $c^2 - k_1^2 - 1 = 1 - 2.25 - 1 = -2.25 < 0$, we enter the parameter regime $c^2 < k_1^2 + 1$, which for $p = 3$ produces a spatially modulated localised wave—a spatially localised wave with internal oscillations—rather than the extended wave train observed for $p = 2$.

The solution exhibits modulated localised wave behaviour (see Fig. 6): A spatially confined wave packet with internal oscillatory structure. Unlike the periodic wave train observed for $p = 2$ (Fig. 4), the $p = 3$ solution remains spatially confined near the origin. This fundamental difference arises from the complex-valued parameter $\lambda = -\sqrt{\sqrt{2}/(i\sqrt{|\Delta|})}$, which has both real and imaginary parts.

The real part of λ creates exponential localisation, confining the wave to a finite spatial region with characteristic decay length $\alpha \approx 1/|\mathrm{Re}(\lambda)|$.

The imaginary part of λ generates rapid oscillations within this localised envelope, with internal wavelength

$$\ell_{\text{internal}} = \frac{2\pi}{|\mathrm{Im}(\lambda)|} \approx 2\pi\sqrt{\frac{2}{|\Delta|}} \approx 5.92.$$

This modulated localised wave structure differs fundamentally from the $p = 2$ case: Instead of a wave train extending throughout space, the $p = 3$ solution remains localised while exhibiting multiple internal oscillations within its envelope. Such structures combine characteristics of envelope solitons with spatial modulation, but maintain a stationary (non-breathing) envelope.

In plasma physics, these structures represent self-trapped Langmuir wave packets with internal spatial modulation while maintaining overall localisation. In nonlinear optics, they correspond to spatially modulated envelope structures in defocusing media, distinct from temporally pulsating spatially modulated localised wave that undergo periodic amplitude oscillations. The multiple internal oscillations within a localised envelope reflect the competing effects of quintic ($p = 3$) nonlinearity and dispersion, mediated by the complex-valued parameter λ.

5.6 Relation to linear stability of uniform states

Although the stability analysis in Sect. 4 concerns *uniform* backgrounds rather than the travelling waves themselves, certain parameter-dependent features provide qualitative insight into the observed solution behaviour:

Localised solutions (Figs. 2, 3 and 5). These profiles emerge in the parameter regime $c^2 > k_1^2 + 1$, where the dispersion relation $m^2 = 2k^2 + 1 + pC_0^{p-1}$ for uniform backgrounds indicates marginal stability with purely real frequencies. This conservative (Hamiltonian) character is consistent with the persistent, non-dispersive propagation of localised structures. The characteristic spatial decay lengths $\alpha = 1/\sqrt{7}$ ($p = 2$) and $\alpha = 1/\sqrt{8.5}$ ($p = 3$) are determined by the balance between nonlinearity and dispersion encoded in the parameter combination $c^2 - k_1^2 - 1$.

Periodic wave trains ($p = 2$, Fig. 4). In the regime $c^2 < k_1^2 + 1$, the argument of hyperbolic functions in solution (15) becomes purely imaginary, transforming them into trigonometric functions. This yields extended periodic structures with wavelength $\ell = 2\pi/\sqrt{|c^2 - k_1^2 - 1|} \approx 11.3$. The transition at $c^2 = k_1^2 + 1$ reflects a qualitative change in the effective dispersion-nonlinearity balance.

Modulated localised waves ($p = 3$, Fig. 6). For $p = 3$ in the regime $c^2 < k_1^2 + 1$, the parameter λ in solution (16) acquires both real and imaginary parts, producing a spatially confined envelope (from $\mathrm{Re}(\lambda)$) with rapid internal oscillations (from $\mathrm{Im}(\lambda)$). The internal wavelength $\ell_{\text{internal}} \approx 5.92$ characterises these oscillations. This differs fundamentally from the extended wave trains observed for $p = 2$, illustrating how higher-order nonlinearities modify the localisation-oscillation interplay.

Regime transition. The critical threshold $c^2 = k_1^2 + 1$ marks a bifurcation in solution character. While the linear

stability analysis of Sect. 4 does not directly govern the stability of these *nonlinear* coherent structures, the parameter $c^2 - k_1^2 - 1$ enters both the dispersion relation for uniform states and the functional form of the travelling waves, suggesting a common underlying mechanism related to the competition between wave propagation speed and effective restoring forces.

Important caveat: The exponential decay rates, spatial profiles, and long-term stability of the localised solutions (15)–(16) are determined by the *nonlinear* structure of these waves, not by the linear analysis of uniform backgrounds. A rigorous stability assessment would require spectral analysis of the linearised operator around each specific wave profile, which lies beyond the present scope.

5.7 Summary of graphical findings

The graphical profiles are fully consistent with the linear stability analysis of Sect. 4. Localised solutions correspond to marginally stable modes with purely imaginary growth rates, while oscillatory solutions exhibit features suggestive of modulational instabilities. Although a definitive assessment of their long-time behaviour requires nonlinear stability analysis, the agreement between analytical predictions and graphical results provides strong validation of the theoretical framework.

6 Conclusion

This work provides a systematic Lie symmetry analysis of the two-dimensional p-defocusing Klein–Gordon equation with general power-law nonlinearity $|q|^{p-1}$, $p > 1$. By deriving the complete seven-dimensional Lie algebra of point symmetries and exploiting its structure through invariant reductions, we have obtained exact travelling wave solutions and analysed their stability properties.

The principal results of this study are:

Regarding the Lie symmetry structure: The full point symmetry algebra has been derived explicitly from determining equations, providing the foundation for systematic reductions via characteristic equations.

Regarding the exact solutions: Explicit travelling wave solutions were obtained for $p = 2$ and $p = 3$ using the $(1/G')$-expansion method. The solutions exhibit qualitatively different behaviours depending on the sign of $c^2 - k_1^2 - 1$: when $c^2 > k_1^2 + 1$, localised solitary waves emerge for both $p = 2$ and $p = 3$; when $c^2 < k_1^2 + 1$, the nonlinearity parameter critically determines the wave structure—extended periodic wave trains for $p = 2$ versus spatially modulated localised wave (waves with internal oscillatory structure) for $p = 3$.

Regarding the stability analysis: Linear stability analysis reveals that solutions are marginally stable in the localised regime, with dispersion relation $\omega^2 = 2k^2 + 1 + pC_0^{p-1}$ providing explicit phase and group velocities.

Regarding the methodological contribution: In contrast to approaches employing ad hoc ansätze, all reductions are derived systematically from the symmetry algebra. This unified framework classifies translation-invariant, Galilean-type, rotational, and phase-invariant reductions within a single structure. The observation that the homogeneous balance number $M = 2/(p-1)$ is non-integer for general p indicates the need for alternative methods beyond $p = 2, 3$.

The solutions admit natural interpretations in plasma physics (envelope solitons and modulated localised waves representing self-trapped Langmuir wave packets with varying internal structure), nonlinear optics (localised pulse structures and spatially modulated envelopes in defocusing Kerr media), and field theory (scalar configurations with varying spatial localisation and internal oscillatory patterns). The threshold $c^2 = k_1^2 + 1$ separates solitary-wave regimes from oscillatory regimes, with the latter exhibiting qualitatively different structures depending on the nonlinearity order: Extended wave trains for $p = 2$ versus spatially modulated localised waves for $p = 3$.

Several directions remain open for investigation: extension to general p via elliptic function methods, nonlinear stability analysis using Lyapunov functionals, derivation of conservation laws via Noether's theorem, and classification of reductions through optimal systems of subalgebras. Numerical simulations and three-dimensional extensions would further validate the analytical predictions and explore solution interactions.

Overall, this study demonstrates that Lie symmetry analysis provides a systematic framework for constructing and classifying solutions to nonlinear Klein–Gordon equations, with clear advantages over heuristic approaches in both completeness and physical transparency.

Acknowledgements The authors thank the editor and reviewers for their insightful comments and helpful suggestions.

Author Contributions G. I. did conceptualisation, methodology investigation, writing—original draft preparation, and writing—reviewing and editing. D. K. contributed to visualisation, supervision, writing—reviewing and editing.

Funding None.

Data Availability No datasets were generated or analysed during the current study.

Code Availability The algebraic computations were performed using Wolfram Mathematica 13. The notebooks are available from the corresponding author upon reasonable request.

Declarations

Ethics approval and consent to participate Not applicable.

Competing interests The authors declare that they have no known competing financial interests or personal relationships that could have appeared to influence the work reported in this paper.

References

1. Fock V (1926) Zur Schrödingerschen Wellenmechanik. Z Phys 38:242–250
2. Fock V (1926) Über die invariante Form der Wellen-und der Bewegungsgleichungen für einen geladenen Massenpunkt. Z Phys 39:226–232
3. Klein O (1926) Quantentheorie und fünfdimensionale Relativitätstheorie. Z Phys 37:895–906
4. Gordon W (1926) Der Comptoneffekt nach der Schrödingerschen Theorie. Z Phys 40(1):117–133
5. Li J, Zhang L (2002) Bifurcations of traveling wave solutions in generalized one-dimensional Klein-Gordon equation. Chaos, Solitons Fractals 14:581–593
6. Zakharov VE (1972) Collapse of Langmuir Waves. Sov Phys JETP 62:1745–1759
7. Chen J, Wu H, Zhu Q (2018) Bäcklund transformation and soliton–cnoidal wave interaction solution for the coupled Klein-Gordon equations. Nonlinear Dyn 91:1949–1961
8. Zhen HL, Tian B, Sun Y, Chai J, Wen XY (2015) Solitons and chaos of the Klein–Gordon–Zakharov system in a high-frequency plasma. Phys Plasmas 22(10):102304
9. Zhang W, Ma W (1999) Explicit solitary wave solutions to generalized one-dimensional Klein-Gordon equations. Appl Math Mech 20:666–674
10. Sassaman R, Biswas A (2010) Topological and non-topological solitons of the Klein-Gordon equations in 1+2 dimensions. Nonlinear Dyn 61:23–28
11. Zhang Z (2008) New exact traveling wave solutions for the nonlinear Klein-Gordon equation. Turk J Phys 32:235–240
12. Kaya D, Sayed SM (2004) A numerical solution of the Klein-Gordon equation and convergence of the decomposition method. Appl Math Comput 156(2):341–353
13. Polat N, Taskesen H (2014) On the existence of global solutions for a nonlinear Klein-Gordon equation. Filomat 28(5):1073–1079
14. Shatah J (1985) Unstable ground state of nonlinear Klein-Gordon equations. Trans Am Math Soc 290:701–710
15. Shatah J (1983) Stable standing waves of non-linear Klein-Gordon equations. Commun Math Phys 91:313–327
16. Shatah J, Strauss W (1985) Instability of nonlinear bound states. Commun Math Phys 100:173–190
17. Brabec T, Krausz F (1997) Nonlinear optical pulse propagation in the single-cycle regime. Phys Rev Lett 78(17):3282
18. Campbell DK, Schonfeld JF, Wingate CA (1983) Resonance structure in kink–antikink interactions in ϕ^4 theory. Physica D 9(1–2):1–32
19. Liebling SL, Palenzuela C (2017) Dynamical boson stars. Living Rev Relativity 20(1):5
20. Strauss WA (1977) Existence of solitary waves in higher dimensions. Commun Math Phys 55:149–162
21. Roy T (2010) Introduction to scattering for radial 3D NLKG below energy norm. J Differ Equ 248(4):893–923
22. Iskenderoglu G, Kaya D (2022) Chirped self-similar pulses and envelope solutions for a nonlinear Schrödinger's in optical fibers using Lie group method. Chaos, Solitons Fractals 162:112453. https://doi.org/10.1016/j.chaos.2022.112453
23. Hussain A, Jhangeer A, Abbas N (2021) Symmetries, conservation laws and dust acoustic solitons of two-temperature ion in inhomogeneous plasma. Int J Geom Methods Mod Phys 18(05):2150071
24. Hussain A, Zia MK, Nisar KS, Vijayakumar V, Khan I (2022) Lie analysis, conserved vectors, nonlinear self-adjoint classification and exact solutions of generalized (N+1)-dimensional nonlinear Boussinesq equation. AIMS Math 7(7):13139–13168
25. Pinar Z, Kocak H (2022) Lie group analysis and exact solutions of nonlinear dispersive equations for porous media. Eur Phys J Plus 137:227. https://doi.org/10.1140/epjp/s13360-022-02406-2
26. Hydon PE (2000) Symmetry methods for differential equations: a beginner's guide. Cambridge Univ, Press
27. Hussain A, Jhangeer A, Abbas N, Khan I, Nisar KS (2021) Solitary wave patterns and conservation laws of fourth-order nonlinear symmetric regularized long-wave equation arising in plasma. Ain Shams Eng J 12:3919–3930
28. Ali MR, Ma WX, Sadat R (2022) Lie symmetry analysis and invariant solutions for (2+1)-dimensional Bogoyavlensky-Konopelchenko equation with variable-coefficient in the wave propagation. J Ocean Eng Sci 7(3):248–254
29. Yokus A (2011) Solutions of some nonlinear partial differential equations and comparison of their solutions, Ph.D. Thesis, Firat Univ., Elazıg
30. Ovsiannikov LV (1982) Group analysis of differential equations. Acad. Press, USA
31. Olver P (2012) Applications of Lie groups to differential equations. Springer Sci, Germany
32. Bluman GW, Anco SC (2002) Symmetry and integration methods for differential equations, Appl Math Sci, Springer, New York
33. Clarkson P, Kruskal M (1989) New similarity reductions of the Boussinesq equation. J Math Phys 30(10):2201–2213
34. Clarkson P (1989) New similarity reductions for the modified Boussinesq equation. J Phys A: Math Gen 22:2355–2367
35. Miller W (1975) Symmetry, Separation of Variables, and Special Functions, Academic Press, 305–351
36. Forhad M, Samsuzzoha M, Akbar MA (2017) The generalized Kudryashov method to obtain exact traveling wave solutions of the PHI-four equation and the Fisher equation. Results Phys 7:4296–4302
37. Shakeel M, Mohyud-Din ST, Iqbal MA (2018) Modified extended exp-function method for a system of nonlinear partial differential equations defined by seismic sea waves, Pramana - J Phys
38. Ji-Huan H, Xu-Hong W (2006) Exp-function method for nonlinear wave equations. Chaos, Solitons Fractals 30(3):700–708
39. Durur H, Yokus A (2021) Exact solutions of the Benney-Luke equation via $(1/G')$-expansion method. Bilecik Şeyh Edebali Univ Sci J 8(1):56–64
40. Agrawal GP (2013) Nonlinear fiber optics, 5th edn. Elsevier, New York
41. Saha M, Sarma AM (2013) Study of modulation instability and solitary waves in nonlinear optical systems, Ph.D. Thesis, Indian Inst of Guwahati
42. Dündar N, Polat N (2021) Local well-posedness for a generalized two-component Degasperis-Procesi system. Int J Open Probl Comput Math 14(2):32–40
43. Dündar N, Polat N (2013) Existence and stability of solitary-wave solutions of a generalized KdV-BBM type equation. J Adv Res Appl Math 5(4):21–30

Springer Nature or its licensor (e.g. a society or other partner) holds exclusive rights to this article under a publishing agreement with the author(s) or other rightsholder(s); author self-archiving of the accepted manuscript version of this article is solely governed by the terms of such publishing agreement and applicable law.